BIOCHEMISTRY
including biophysical chemistry & molecular biology

Article

pubs.acs.org/biochemistry

Reactions of Cg10062, a *cis*-3-Chloroacrylic Acid Dehalogenase Homologue, with Acetylene and Allene Substrates: Evidence for a Hydration-Dependent Decarboxylation

Jamison P. Huddleston, William H. Johnson, Jr., Gottfried K. Schroeder, and Christian P. Whitman*

Division of Medicinal Chemistry, College of Pharmacy, University of Texas, Austin, Texas 78712, United States

ABSTRACT: Cg10062 is a *cis*-3-chloroacrylic acid dehalogenase (*cis*-CaaD) homologue from *Corynebacterium glutamicum* with an unknown function and an uninformative genomic context. It shares 53% pairwise sequence similarity with *cis*-CaaD including the six active site amino acids (Pro-1, His-28, Arg-70, Arg-73, Tyr-103, and Glu-114) that are critical for *cis*-CaaD activity. However, Cg10062 is a poor *cis*-CaaD: it lacks catalytic efficiency and isomer specificity. Two acetylene compounds (propiolate and 2-butynoate) and an allene compound, 2,3-butadienoate, were investigated as potential substrates. Cg10062 functions as a hydratase/decarboxylase using propiolate as well as the *cis*-3-chloro- and 3-bromoacrylates, generating mixtures of malonate semialdehyde and acetaldehyde. The two activities occur sequentially at the active site using the initial substrate. With 2,3-butadienoate and 2-butynoate, Cg10062 functions as a hydratase and converts both to acetoacetate. Mutations of the proposed water-activating residues (E114Q, E114D, and Y103F) have a range of consequences from a reduction in wild type activity to a switch of activities (i.e., hydratase into a hydratase/decarboxylase or vice versa). The intermediates for the hydration and decarboxylation products can be trapped as covalent adducts to Pro-1 when $NaCNBH_3$ is incubated with the E114D mutant and 2,3-butadienoate or 2-butynoate, and the Y103F mutant and 2-butynoate. Three mechanisms are presented to explain these findings. One mechanism involves the direct attack of water on the substrate, whereas the other two mechanisms use covalent catalysis in which a covalent bond forms between Pro-1 and the hydration product or the substrate. The strengths and weaknesses of the mechanisms and the implications for Cg10062 function are discussed.

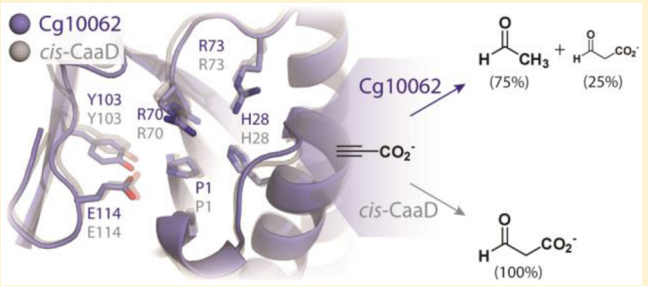

Cg10062 is a 149-amino acid protein from *Corynebacterium glutamicum* with unknown biological function(s).[1,2] It is a *cis*-3-chloroacrylic acid dehalogenase (*cis*-CaaD) homologue (~34% pairwise sequence identity and 53% similarity) and is categorized in the *cis*-CaaD family, one of the five known families in the tautomerase superfamily.[3−5] Members of this superfamily share a characteristic $\beta-\alpha-\beta$ fold and a catalytic amino-terminal proline.

In contrast to Cg10062, *cis*-CaaD from *Pseudomonas pavonaceae* 170 carries out a known reaction in an established pathway.[3,6−8] The enzyme catalyzes the hydrolytic dehalogenation of *cis*-3-chloroacrylate (**2**, Scheme 1) to produce malonate semialdehyde (**4**).[3] A related enzyme, *trans*-3-chloroacrylic acid dehalogenase (CaaD), processes the *trans* isomer, **3**, to **4**.[9] A subsequent decarboxylation reaction catalyzed by malonate semialdehyde decarboxylase (MSAD) yields acetaldehyde (**5**), which is presumably shuttled to the Krebs cycle.[10] These reactions are two of the five steps that convert the isomeric mixture of the nematicide, 1,3-dichloropropene (**1**), to acetaldehyde.[6−8]

Cg10062 and *cis*-CaaD share common features.[1,2,11,12] Both are homotrimers where each monomer is composed of 149 amino acids. Six residues critical for *cis*-CaaD activity (Pro-1, His-28, Arg-70, Arg-73, Tyr-103, and Glu-114) are also present in Cg10062.[1] Moreover, the structures and active site regions are largely superimposable including the position of the six key residues.[11,12] However, Cg10062 is not a very efficient *cis*-CaaD: there is a significant reduction in k_{cat}/K_m (~1000-fold using *cis*-3-bromoacrylate), and it processes both the *cis* and *trans* isomers of 3-chloroacrylate with a preference for the *cis* isomer.[1,2,11] In contrast, *cis*-CaaD and CaaD are highly specific for their respective isomers.[1,3,13]

The basis for these differences is not known. The substantial increase in K_m (~687-fold) observed for Cg10062 using (*cis*-3-bromoacrylate) suggests that it might originate in the elements that govern substrate specificity.[11,12] Two possibilities include the more spacious active site of Cg10062 or a six-residue loop in *cis*-CaaD that is observed closed down on the active site in the crystal structure of the enzyme inactivated by an irreversible inhibitor.[11] A similar feature has not been observed in Cg10062. Both possibilities have been explored, but the results of these studies did not provide a definite explanation.

In the course of our work on *cis*-CaaD, CaaD, and Cg10062, we desired a halide-free solution of **4**, which could only be

Received: March 5, 2015
Revised: April 17, 2015
Published: April 20, 2015

DOI: 10.1021/acs.biochem.5b00240
Biochemistry 2015, 54, 3009−3023

Scheme 1. Enzyme-Catalyzed Reactions Comprising the 1,3-Dichloropropene Catabolic Pathway

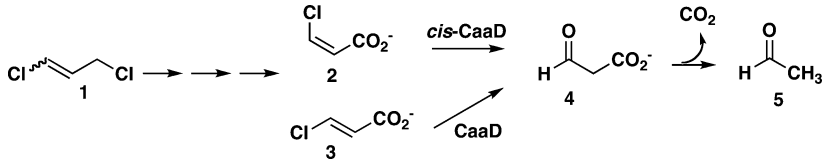

generated with halide from **2** or **3** using the appropriate dehalogenase.[10] It is known that all three enzymes hydrate the acetylene compound, 2-oxo-3-pentynoate (**6**, Scheme 2A), to produce acetopyruvate (**7**) with varying degrees of efficiency (CaaD ≫ Cg10062 > *cis*-CaaD).[1,3,13] This observation prompted us to incubate *cis*-CaaD with propiolate (**8**, Scheme 2B), which was anticipated to produce **4** upon hydration. Indeed, **8** is a reasonably good substrate for *cis*-CaaD (k_{cat}/K_m = 6.4 × 10^3 M^{-1} s^{-1}) but an even better one for Cg10062. Interestingly, an analysis showed that **4** is only a minor product of the Cg10062-catalyzed reaction. Instead, a mixture of **4** and **5** was obtained (25% and 75%, respectively), suggesting that Cg10062 functions as both a hydratase and decarboxylase (Scheme 3).

These findings prompted a detailed investigation of this reaction with the wild type enzyme and active site mutants and confirmed that the hydration and decarboxylation reactions take place at the same active site. The reactions also appear to occur sequentially using the initial substrate (i.e., **8**), because the enzyme does not decarboxylate exogenously added **4**. The reactions of Cg10062 with 2,3-butadienoate (**9**) and 2-butynoate (**10**), as well as those of Cg10062 with **2** and **3**, were also examined. For **3**, **9**, and **10**, Cg10062 functions as a hydratase. With **2**, Cg10062 is a hydratase/decarboxylase, but it is not as efficient as with **8** (as assessed by the k_{cat}/K_m values). A mutational analysis of two water-activating residues (Glu-114 and Tyr-103) provided an interesting array of results. There was a reduction in wild type activity for some mutant/substrate combinations, as would be expected, but other combinations switched activities (hydratase to hydratase/decarboxylase or vice versa). Moreover, the likely intermediates of the hydration and decarboxylation products can be trapped (using $NaCNBH_3$) covalently attached to Pro-1 for the E114D mutant with **9** and **10** and the Y103F mutant with **10**. Three mechanisms are proposed to account for these observations. One mechanism involves a direct attack of water on the substrate followed by the decarboxylation of some of the hydration products. In a second mechanism, the substrate undergoes hydration, which is followed in some cases by the formation of a Schiff base between the hydration product and Pro-1. Decarboxylation and hydrolysis of the Schiff base complete the reaction. A third mechanism involves the partitioning of the different substrates between covalent catalysis through Pro-1 and the direct attack of water. The route might be determined by the substrate's orientation in the active site with respect to Pro-1 and two water-activating residues (i.e., Glu-114 and Tyr-103). Finally, the possible biological relevance of the reaction of Cg10062 with **8**, the best substrate for Cg10062 identified to date, is discussed.

Scheme 2. (A) Enzyme-Catalyzed Conversion of 2-Oxo-3-pentynoate (6) to Acetopyruvate (7) and (B) Acetylene and Allene Substrates Used in This Work

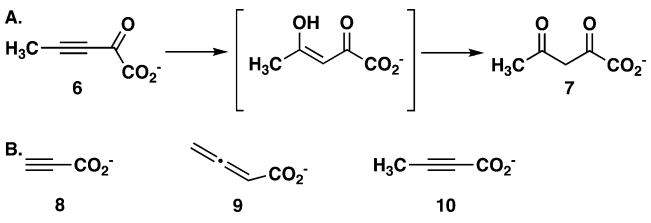

Scheme 3. Cg10062-Catalyzed Conversion of Propiolate (8) to a Mixture of Malonate Semialdehyde (4) and Acetaldehyde (5)

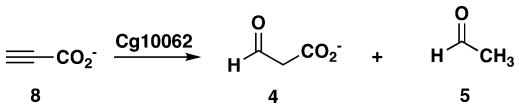

EXPERIMENTAL PROCEDURES

Materials. Chemicals, biochemicals, buffers, and solvents were purchased from Sigma-Aldrich Chemical Co. (St. Louis, MO), Fisher Scientific Inc. (Pittsburgh, PA), Fluka Chemical Corp. (Milwaukee, WI), or EMD Millipore, Inc. (Billerica, MA). Sodium phosphate buffer salts were at least 99.99% pure or greater, as indicated by the manufacturer. Propiolic acid (98%, **8**) and 2-butynoate (**10**) were purchased from Sigma-Aldrich. Both were purified further prior to use by distillation (**8**) or recrystallization (**10**). 2,3-Butadienoate (**9**) was synthesized according to published methods.[14] The DEAE-Sepharose and Phenyl-Sepharose 6 Fast Flow resins used for protein purification were obtained from Sigma-Aldrich Chemical Co. (St Louis, MO). The Econo-Column chromatography columns were obtained from BioRad (Hercules, CA). The Amicon stirred cell concentrators and the ultrafiltration membranes (10000 Da, MW cutoff) were purchased from EMD Millipore Inc. Malonate semialdehyde decarboxylase (MSAD) was purified as described previously.[10]

Bacterial Strains, Plasmids, and Growth Conditions. *Escherichia coli* strain BL21-Gold(DE3) was obtained from Agilent Technologies (Santa Clara, CA). The *E. coli* DH5α cells were obtained from Invitrogen (Carlsbad, CA). Cells were grown at 37 °C overnight in Luria−Bertani (LB) media that contained ampicillin (Ap, 100 μg/mL).

General Methods. The PCR amplification of DNA sequences was conducted in a GeneAmp 2700 thermocycler (Applied Biosystems, Carlsbad, CA). Techniques for restriction enzyme digestion, ligation, transformation, and other standard molecular biology manipulations were based on methods described elsewhere.[15] DNA sequencing was performed in the DNA Core Facility in the Institute for Cellular and Molecular Biology (ICMB) at the University of Texas at Austin. Electrospray ionization mass spectrometry (ESI-MS) was carried out on an LCQ electrospray ion-trap mass spectrometer (Thermo, San Jose, CA). Peptide fragment masses were determined using Voyager-DE Pro matrix-assisted laser desorption/ionization (MALDI) mass spectrometer run in

DOI: 10.1021/acs.biochem.5b00240
Biochemistry 2015, 54, 3009−3023

the linear mode. Both instruments are housed in the ICMB Protein and Metabolite Analysis Facility at the University of Texas. Steady-state kinetic assays were performed on an Agilent 8453 diode-array spectrophotometer at 22 °C. Nonlinear regression data analysis was performed using the program Grafit (Erithacus Software Ltd., Staines, U.K.). Protein concentrations were determined by the Waddell method.[16] Sodium dodecyl sulfate-polyacrylamide gel electrophoresis (SDS-PAGE) was carried out on denaturing gels containing 12% polyacrylamide.[17] Nuclear magnetic resonance (NMR) spectra were recorded on a Varian INOVA-500 or a Varian DirectDrive 600 MHz spectrometer (Palo Alto, CA). NMR signals were analyzed using the software program SpinWorks 3.1.6 (Copyright 2009 Kirk Marat, University of Manitoba).

Construction of the Cg10062 Mutants and Expression and Purification of Wild-type and Cg10062 Mutants. The expression vectors for Cg10062 and the P1A, R70A, and E114Q mutants of Cg10062 were constructed as described elsewhere.[1,18] The remaining Cg10062 mutants were constructed using the QuikChange Site-Directed Mutagenesis Kit (Agilent Technologies) following the manufacturer's instructions. Oligonucleotide primers (coding and complementary) were obtained from Sigma-Aldrich. The forward and reverse primers used to introduce the Y103F mutation were 5′-CCAATGAAGAAGTATGGGTATTTATAACGGAGATTCCTGGTTC-3′ and 5′-GAACCAGGAATCTCCGTTATAAATACCCATACTTCTTCATTGG-3′, respectively. The forward and reverse primers used to introduce the E114D mutation were 5′-GGTTCCAATATGACGGATTATGGCCGTCTCCTCAT-3′ and 5′-ATGAGGAGACGGCCATAATCCGGTCATATTGGAACC-3′, respectively. The codon used to introduce the mutation is underlined in each primer. The E114Q/Y103F double mutant of Cg10062 was constructed by the QuikChange method using the E114Q-pET3b plasmid as template DNA and the primers used for the Y103F mutant. Wild-type Cg10062 and the mutants were grown and expressed in *E. coli* BL21-Gold(DE3) cells and purified by previously published protocols.[1,2,18]

Mass Spectral Analysis of Cg10062 and the Cg10062 Mutants. The molecular masses of Cg10062 and mutants were determined by deconvolution of the ESI-MS spectra. Samples for analysis were made 1 mg/mL, as described elsewhere.[13] The observed monomeric molecular masses (MH^+) for the wild-type enzyme, and the E114Q-, E114D-, Y103F-, and P1A-Cg10062 mutants are 17100, 17098, 17085, 17085, and 17072 Da, respectively. These masses agree with the calculated masses (within experimental error).

Steady State Kinetics. The assays were carried out at 22 °C in 100 mM Na_2HPO_4 buffer, pH 8.1, using various concentrations of enzyme (0.02−2 μM) depending on the k_{cat} of the enzyme with the substrate. A stock solution of **8** (~400 mg/mL, 5.71 M) was made up by pipetting (with a disposable glass pipet) ~0.34 g (~0.34 mL) of liquid **8** into 100 mM tribasic phosphate buffer (0.5 mL). The final pH of this stock solution is ~3.5. A 100 mM propiolate solution was made up from this stock solution using a mixture of a 100 mM tribasic and dibasic phosphate buffer so that the final pH was 8.1. Diluted enzyme solutions were equilibrated for 1 h before the assays. Initial rates were plotted vs substrate concentration and fit to the Michaelis−Menten equation using Grafit to determine k_{cat} and K_m. The reported errors are calculated from the standard deviations of the fit to the data. If saturation kinetics were not observed, the collected data were fit to a straight line where the slope is equal to k_{cat}/K_m.[19] The reactions of **2**, **3**, and **8** were monitored by a coupled assay described elsewhere, where the reduction of acetaldehyde by alcohol dehydrogenase is coupled to the oxidation of NADH.[1,10,11] Cg10062 processes *cis*-3-bromoacrylate with comparable kinetic parameters and product ratios to those determined for **2** (data not shown). The hydration of **9** to acetoacetate (**11**) was followed by monitoring the decrease in absorbance at 224 nm (ε_{224} = 1125 μM^{-1} cm^{-1}), as described previously.[11] The hydration of **10** to acetoacetate (**11**, Scheme 4) was followed by monitoring the decrease in absorbance at 220 nm (ε_{220} = 624 μM^{-1} cm^{-1}). The decarboxylase activity of Cg10062 and the mutants with **2**, **3**, or **8** (yielding **5**) was determined using the coupled assay described above where MSAD was excluded from the mixture and by ^1H NMR spectroscopy. The decarboxylase activity of Cg10062 and mutants with **9** or **10** (yielding acetone, **12**) was determined by ^1H NMR spectroscopy.

Decarboxylation of 4 and 11 by Cg10062 and Mutants. Malonate semialdehyde (**4**, 10−80 mM) was generated using *cis*-CaaD and *cis*-3-chloroacrylate (**2**), as previously reported.[10,20] The decarboxylation of exogenous **4** by Cg10062 and the mutants was monitored by the coupled assay (above) without MSAD and by ^1H NMR spectroscopy.

Identification of the Products of the Cg10062- and Mutant-Catalyzed Reactions with 2, 3, 4, 8, 9, and 10 by ^1H NMR Spectroscopy. The protocol for monitoring the reaction of Cg10062 with **2** or **3** by ^1H NMR spectroscopy is described elsewhere.[1] The same procedure was used with the following modifications for monitoring the reaction of Cg10062 with **8**, **9**, or **10**. Accordingly, an amount of **8**, **9**, or **10** (4 mg, ~95 mM for **8** and ~80 mM for **9** and **10**) was added to 100 mM Na_2HPO_4 buffer (pH 9.2) containing 30 μL of DMSO-d_6 (final total volume of 600 μL). The final pH of the solution was adjusted to 8.0. Subsequently, a 7-μL aliquot of enzyme (wild-type or the E114Q, E114D, Y103F, Y103F/E114Q, and P1A mutant of Cg10062, from 18 mg/mL, 15 mg/mL, 17 mg/mL, 28 mg/mL, 16 mg/mL, or 17 mg/mL stock solutions, respectively) was added to the mixture, and product formation was monitored every 3 min over a 3−90 min time interval depending on the enzymatic activity. DMSO-d_6 was used as the lock signal and for the standardization of the chemical shifts (at 2.49 ppm). The chemical shifts for **4**, **5**, their hydrates, **11**, and **12** are reported elsewhere.[13,21] The approximate amount of product in the mixtures was determined by integration, as described previously.[1]

ESI-MS Analysis of $NaCNBH_3$-Treated Mixtures Containing the Y103F or E114D Mutants of Cg10062 and 9 or 10. Six reaction mixtures (300 μL) were made up containing 100 mM Na_2HPO_4 buffer (37 μL, pH 8.0), $NaCNBH_3$ (50 μL of a 1.6 M solution in 100 mM Na_2HPO_4, pH 8.0), and the Y103F or E114D mutant of Cg10062 (20 μL) (3 reaction mixtures each). After a 10 min incubation period, **9** or **10** (193 μL from a 14 mg/mL stock solution initially made up in 100 mM Na_3PO_4 buffer with the final pH adjusted to 8.0 using a 50% NaOH solution) was added to the mixtures containing the

Scheme 4. Cg10062-Catalyzed Conversion of 2-Butynoate (10) to a Mixture of Acetoacetate (11) and Acetone (12)

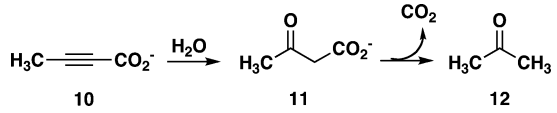

DOI: 10.1021/acs.biochem.5b00240
Biochemistry 2015, 54, 3009−3023

Y103F- or E114D-Cg10062 (accounting for four of the six reaction mixtures). The remaining two mixtures (one with the Y103F mutant and one with the E114D mutant) served as controls where the substrate is replaced with 100 mM Na_2HPO_4 buffer, pH 8.0 (193 μL). The reaction mixtures incubated overnight at room temperature. Subsequently, the remaining hydratase activity in each sample (using **9** as substrate) was determined by the UV assay described previously.[11] The activities of three of the four reaction mixtures (**9** with E114D-Cg10062 and **10** with Y103F- and E114D-Cg10062) were reduced 10−100-fold from those observed in the control reaction mixtures. The incubation of **9** with Y103F-Cg10062 results in no reduction of activity from that observed in the control sample. The mixtures with reduced activity (i.e., **9** with E114D-Cg10062 and **10** with Y103F- and E114D-Cg10062) were then prepared for ESI-MS analysis, as described elsewhere.[3,21] Four additional reaction mixtures were set up that contained the Y103F and E114D mutants of Cg10062 along with exogenous **11** or **12**. Following the protocol described above, an aliquot (230 μL) of **11** or **12** (from a 0.14 M stock solution, 14.95 and 8.02 mg/mL, respectively) was added to 70 μL of preincubated solution containing enzyme (20 μL of the Y103F or E114D mutant of Cg10062) and $NaCNBH_3$ (50 μL). There was no reduction in the activity of these samples, as assessed by an assay using **9** (compared with that of control), so that ESI-MS analysis was not carried out on these samples.

Peptide Mapping and MALDI-MS Analysis. The covalently modified Y103F and E114D mutants of Cg10062 (by their incubation with **9** and **10** and treatment with $NaCNBH_3$) were treated with a solution of *Staphylococcus aureus* endoproteinase Glu-C (protease V-8), following a previously published protocol.[3,21] After a 48-h incubation period, the resulting peptide mixture was analyzed by MALDI-MS, as described previously.[3,21]

RESULTS

Kinetic Parameters of Cg10062 with 8 and 10. The steady-state kinetic parameters were measured for Cg10062 with the acetylene compounds, **2**, **8**, and **10**, and are summarized with those previously measured for Cg10062 with **3** and **9** in Table 1.[1,11,18] Cg10062 shows the highest k_{cat} and lowest K_m values with propiolate (**8**), yielding a k_{cat}/K_m value of 1.8×10^5 M^{-1} s^{-1}. This k_{cat}/K_m is 12000-fold and 6000-fold higher than those measured respectively for **2** and 2-butynoate (**10**), and 35-fold higher than the one measured for 2,3-butadienoate (**9**). The k_{cat}/K_m values for Cg10062 with **2** and **10** are comparable, but the accuracy is limited by the inability to achieve saturation with substrate. Cg10062 has the poorest activity and lowest efficiency with **3**. However, the ability of Cg10062 to process **3** is interesting in light of the inability of *cis*-CaaD to process **3** coupled with the many similarities between *cis*-CaaD and Cg10062.

Table 1. Steady-state Kinetic Parameters for the Cg10062-catalyzed Reactions[a]

sub	K_m (μM)	k_{cat} (s^{-1})	k_{cat}/K_m (M^{-1} s^{-1})
2	72000 ± 8500	1 ± 0.1	14 ± 2
3[b]	78000 ± 36000	0.06 ± 0.01	0.8 ± 0.4
8	33 ± 5	6 ± 0.2	$(1.8 \pm 0.2) \times 10^5$
9[c]	780 ± 120	4 ± 0.3	$(5.1 \pm 0.8) \times 10^3$
10[d]			30 ± 2

[a]The kinetic parameters for **8** and **10** were measured by the assay described in the text in 100 mM Na_2HPO_4 buffer (pH 8) at 22 °C. [b]Reported in refs 1 and 18. [c]Reported in ref 11. [d]Saturation kinetics could not be achieved with **10**. The initial rates were plotted versus [**10**] and fit to a straight line to provide a value for k_{cat}/K_m.[19]

^{1}H NMR Characterization of the Cg10062-Catalyzed Reaction with 2, 3, 4, 8, 9, and 10. ^{1}H NMR spectroscopic analysis of the reaction of Cg10062 with **8** showed that **5** is the major product (~75%) of the reaction along with **4** (~25%) (Figure 1A). The reaction is complete in less than 3 min, indicating that **5** does not result from the nonenzymatic decarboxylation of **4**. The same kinetic parameters are obtained with and without MSAD in the coupled assay, which is also consistent with **5** being the major product. The subsequent incubation of Cg10062 with exogenously generated **4** (10−80 mM) did not produce **5** at a rate faster than that observed for the nonenzymatic rate, as assessed by UV and ^{1}H NMR spectroscopy. On the basis of these observations, Cg10062 catalyzes the hydration-dependent decarboxylation of **8**.

These observations prompted a closer examination of the reactions of Cg10062 with **2** and **3** by ^{1}H NMR spectroscopy. Cg10062 converts **2** to both **4** (7%) and **5** (33%) after 48 min with 60% of **2** remaining (Figure 1B). (Two doublets corresponding to the protons of **2** appear at 6.11 and 6.19 ppm, which are outside the range shown in the figure.[3]) Although **3** is converted to **4** (2.9%) by Cg10062, **4** is not processed to **5** by the enzyme after 48 min (Figure 1C). A small amount of acetaldehyde, **5**, is observed (1.5%), but this is due to the nonenzymatic decarboxylation of **4** in the course of the 48 min incubation time. This was confirmed by the UV assay (data not shown). A large amount of unreacted substrate (95.6%) is also present. (Two doublets for the protons of **3** appear at 6.09 and 6.89 ppm, which are outside the range shown in the figure.[13]) The presence of **5** in the reaction of Cg10062 with **2** was noted previously but was attributed to a nonenzymatic process or a promiscuous decarboxylase activity of Cg10062.[1]

With **9** and **10**, Cg10062 functions as a hydratase.[11] The reaction of Cg10062 with **9** is complete in less than 3 min, and the ^{1}H NMR spectrum shows mostly **11**, which results from the hydration of **9** (Figure 1D). The reaction of **10** with Cg10062 yields a similar result, but over a longer time period: it is complete after 39 min, and **11** is the major product observed (Figure 1E). There is a small amount of **12** present (~2.5% after 18 min), which exceeds the expected amount from the nonenzymatic decarboxylation of **11**. Hence, Cg10062 functions primarily as a hydratase with this substrate, but has a weak decarboxylase activity.

Incubation of the P1A, R70A, and Y103F/E114Q Mutants of Cg10062 with 2, 8, 9, and 10. In order to assess whether the reactions are taking place at the active site of Cg10062 (or another site), various active site mutants were examined with **2**, **8**, **9**, and **10**. The P1A mutant was examined with **2**, **8**, and **10**. The R70A mutant was examined with **2**, **8**, and **9**. The Y103F/E114Q mutant was examined with **8** and **9**. (The reactions of the P1A and R73A mutants of Cg10062 with **3** were previously reported.[1]) In all cases, the product signals were greatly reduced in the ^{1}H NMR spectra (data not shown). These observations suggest that the reactions take place in the same active site.

Kinetic Parameters of E114Q-Cg10062 with 2, 8, and 9. The steady-state kinetic parameters for the E114Q mutant of

DOI: 10.1021/acs.biochem.5b00240
Biochemistry 2015, 54, 3009−3023

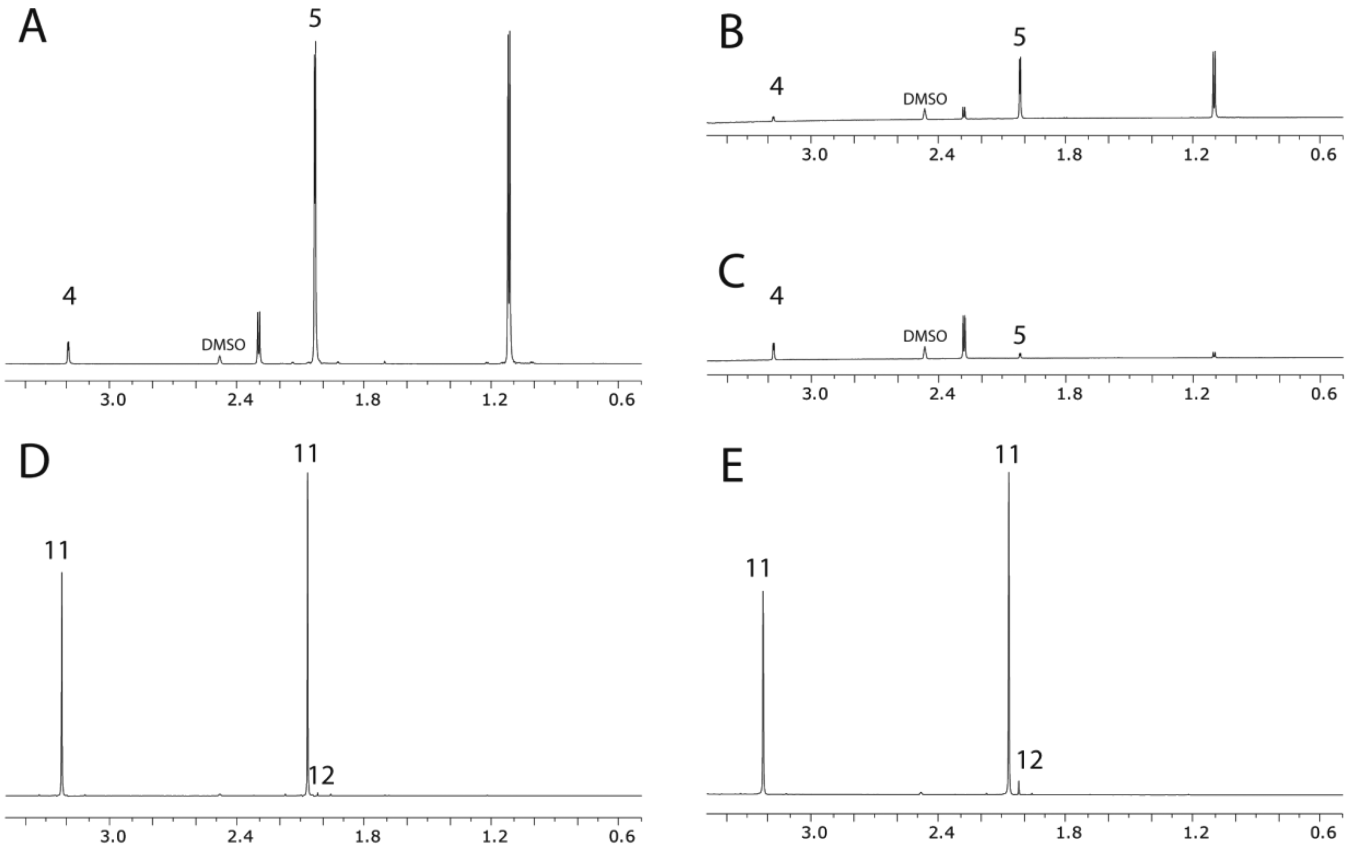

Figure 1. ^{1}H NMR spectroscopic product analysis of the reaction of Cg10062 with **2**, **3**, **8**, **9**, or **10**. (A) Products of Cg10062 with **8** (~95 mM) after 3 min. (B) Products of Cg10062 with **2** (~63 mM) after 48 min. The signals for the unreacted **2** are not shown. (C) Products of Cg10062 with **3** (~63 mM) after 48 min. The signals for the unreacted **3** are not shown. The small amount of **5** present is consistent with nonenzymatic decarboxylation of **4**. (D) Products of Cg10062 with **9** (~80 mM) after 3 min. The small amount of **12** present is consistent with the nonenzymatic decarboxylation of **11**. (E) Products of Cg10062 with **10** (~80 mM) after 39 min. The amount of **12** present (2.5%) is more than expected for nonenzymatic decarboxylation. All reactions contained ~12.3 μM Cg10062 and 30 μL of DMSO-d_6. The reactions are individually scaled to show the products of the reactions. The scale can be assessed by the height of the DMSO peak (labeled in the spectra). The hydrates of **4** and **5** are also present: the signal at ~2.3 ppm corresponds to the methyl group of the hydrate of **4**, and the signal at ~1.1 ppm corresponds to the methyl group of the hydrate of **5**.[13]

Cg10062 with **2**, **8**, and **9** are summarized in Table 2. With **8**, the E114Q mutant of Cg10062 shows a 7.5-fold reduction in k_{cat} (vs wild type) and an 11-fold reduction in K_m. As a result, there is a slight increase in the value of k_{cat}/K_m. With **9**, the k_{cat}/K_m value increases ~5-fold, which is due to an increase in the k_{cat}. Like **8**, the E114Q mutant of Cg10062 shows a reduction in both the k_{cat} and K_m values using **2** and results in a slightly higher k_{cat}/K_m (vs wild type). The steady-state kinetic parameters for the E114Q mutant using **3** or **10** could not be determined with the coupled assay because the reactions are too slow. Although the k_{cat}/K_m values for the E114Q mutant with **2** and **8** are comparable with the respective ones for wild type, the E114Q mutant does not carry out a decarboxylation reaction with the hydration product, and MSAD must be present in the assay mixture in order to monitor the reactions by the UV assay.

Table 2. Steady-State Kinetic Parameters for the E114Q-Cg10062-Catalyzed Reactions[a]

	K_m (μM)	k_{cat} (s^{-1})	k_{cat}/K_m (M^{-1} s^{-1})
2	4000 ± 800	0.4 ± 0.05	100 ± 25
8	3 ± 0.25	0.80 ± 0.02	(2.7 ± 0.2) × 10^5
9	660 ± 75	16 ± 1	(2.4 ± 0.3) × 10^4

[a]The kinetic parameters were measured using the assay described in the text in 100 mM Na_2HPO_4 buffer (pH 8) at 22 °C.

^{1}H NMR Characterization of the E114Q-Cg10062-Catalyzed Reaction with 2, 3, 8, 9, and 10. ^{1}H NMR analysis of the five E114Q-Cg10062-catalyzed reactions uncovered some intriguing contrasts to the wild type reactions. With **8**, the E114Q-Cg10062 apparently functions as a hydratase because **4** is now the major product (8.5%) of the reaction after 18 min (Figure 2A). A small amount of **5** (0.5%) is observed in the NMR spectrum, but it is similar to that observed for the nonenzymatic decarboxylation of **4**. (This was confirmed by the UV assay using MSAD.) There is also a large amount of unreacted substrate present (91%), indicated by the singlet at ~2.9 ppm. A similar result is observed when **2** is incubated with E114Q-Cg10062 (Figure 2B). After 18 min, the mixture consists of unreacted substrate (80%), **4** (19%), and a small amount of **5** (1%). The E114Q mutant of Cg10062 does not process **3** to any significant extent after 90 min (Figure 2C).

With **9** and **10**, the ^{1}H NMR analysis suggests that the E114Q mutant of Cg10062 functions as a hydratase/decarboxylase. With **9**, the E114Q-Cg10062-catalyzed reaction is complete after 12 min, and yields mostly **11** (83%) with a significant amount of **12** present (~17%) (Figure 2D).

DOI: 10.1021/acs.biochem.5b00240
Biochemistry 2015, 54, 3009−3023

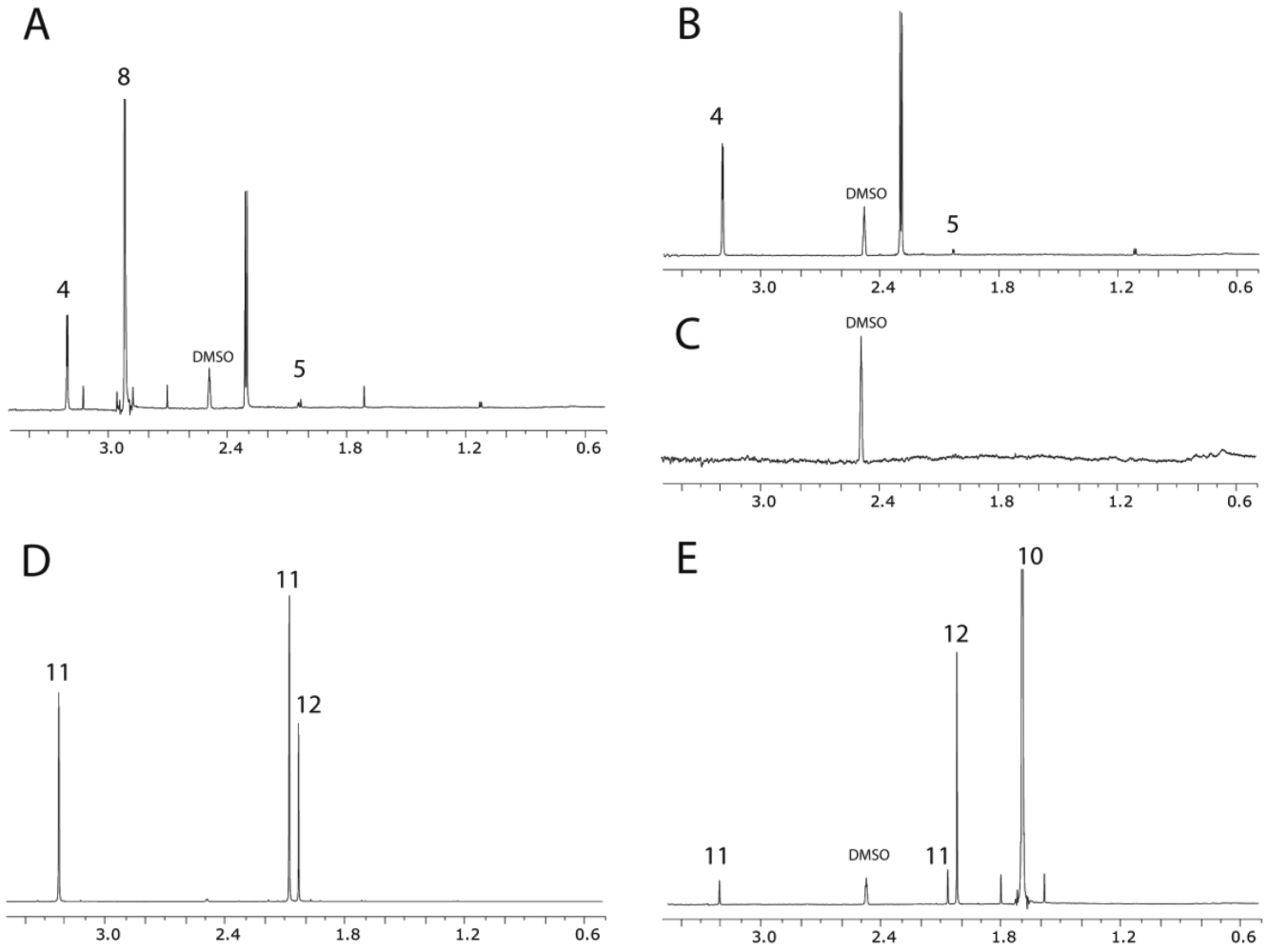

Figure 2. [1]H NMR spectroscopic product analysis of the reaction of E114Q-Cg10062 with **2**, **3**, **8**, **9**, or **10**. (A) Products of E114Q-Cg10062 with **8** (~95 mM) after 18 min. The small amount of **5** present is consistent with nonenzymatic decarboxylation of **4**. The reaction is not complete with a significant amount of **8** present (identified by the singlet at 2.90 ppm). (B) Products of E114Q-Cg10062 with **2** (~63 mM) after 18 min. The small amount of **5** present is consistent with nonenzymatic decarboxylation of **4**. The reaction is not complete with a significant amount of **2** still present (NMR signals not shown). (C) Products of E114Q-Cg10062 with **3** (~63 mM) after 90 min. There are no observable signals for **4** or **5**. (D) Products of E114Q-Cg10062 with **9** (~80 mM) after 12 min. The signal at 2.03 ppm corresponds to the methyl group of **12**. The signals at 2.08 and 3.23 ppm correspond to the methyl and methylene groups respectively of **11**.[21] (E) Products of E114Q-Cg10062 with **10** (~80 mM) after 90 min. All reactions contained ~12.3 μM E114Q-Cg10062 and 30 μL of DMSO-d_6. The reactions are individually scaled to show the product reaction. The scale can be assessed by the height of the DMSO peak, which is labeled in the spectra.

Moreover, there is no further change in the amounts of **11** or **12** after the reaction mixtures incubate for an additional 15 min. This suggests that the E114Q mutant does not catalyze the decarboxylation of **11** when added exogenously, just as wild-type does not catalyze the decarboxylation of **4** (at a rate faster than nonenzymatic) when added exogenously. With **10**, the E114Q-Cg10062-catalyzed reaction produces **12** (2.2%, which is 73% of the total products observed) as the major product and **11** as the minor product (0.8%, which is 27% of the total products observed) after 90 min (Figure 2E). A large amount of unreacted substrate remains (97%), as indicated by the singlet at ~1.7 ppm. These results suggest that the E114Q mutant catalyzes a decarboxylation reaction (preceded by a hydration reaction), but only using **9** and **10** where the decarboxylation product is **12**.

Kinetic Parameters of E114D-Cg10062 with 2, 8, 9, and 10. The steady state kinetic parameters for the E114D mutant of Cg10062 with **2**, **8**, **9**, and **10** are summarized in Table 3. Using **8**, there is a 6-fold reduction in k_{cat} and a 2.7-fold increase in K_m (vs wild type), which results in a 16-fold decrease in the k_{cat}/K_m. The resulting k_{cat}/K_m (1.1×10^4 M^{-1} s^{-1}) is an order of magnitude less than that measured for wild type. With **2**, the E114D-Cg10062 exhibits poor activity. With **3**, the activity is so poor that it is not possible to measure kinetic parameters. The k_{cat}/K_m for the E114D mutant of Cg10062 using **9** increased slightly from that observed for wild type. The k_{cat}/K_m for the E114D mutant of Cg10062 with **10** is

Table 3. Steady-State Kinetic Parameters for the E114D-Cg10062-Catalyzed Reactions[a]

	K_m (μM)	k_{cat} (s^{-1})	k_{cat}/K_m (M^{-1} s^{-1})
2	40100 ± 10000	0.1 ± 0.02	2.5 ± 0.8
8	90 ± 13	1 ± 0.05	$(1.1 \pm 0.2) \times 10^4$
9	480 ± 86	3.2 ± 0.4	$(6.6 \pm 1.5) \times 10^3$
10	1365 ± 170	0.5 ± 0.03	$(4.1 \pm 0.5) \times 10^2$

[a]The kinetic parameters were measured by the assay described in the text in 100 mM Na_2HPO_4 buffer (pH 8) at 22 °C.

DOI: 10.1021/acs.biochem.5b00240
Biochemistry 2015, 54, 3009−3023

14-fold higher than that for wild type. The k_{cat} is low (0.5 s^{-1}), but a K_m value can be measured unlike the wild type enzyme where saturation kinetics could not be achieved.

^{1}H NMR Characterization of the E114D-Cg10062-Catalyzed Reaction with 8, 9, and 10. The reactions of the E114D mutant of Cg10062 with **8**, **9**, and **10** were monitored by ^{1}H NMR spectroscopy. The major product of the reaction with **8** is **4** (22%), and not **5** (1%) after 3 min (Figure 3A). A significant amount of unreacted substrate (77%) remains (i.e., singlet at ∼2.9 ppm). The E114D mutant of Cg10062 with **9** yields mostly **11** (97.2%) and a small amount of **12** (2.8%) after 3 min (Figure 3B). Similar observations are made for the reaction of **10** with the E114D mutant of Cg10062 (i.e., 91.5% of **11** and 2.5% of **12** and 8.2% unreacted substrate) after 3 min (Figure 3C). These results indicate that the E114D mutant of Cg10062 functions mostly as a hydratase with **9** and **10**, but also has a weak decarboxylase activity.

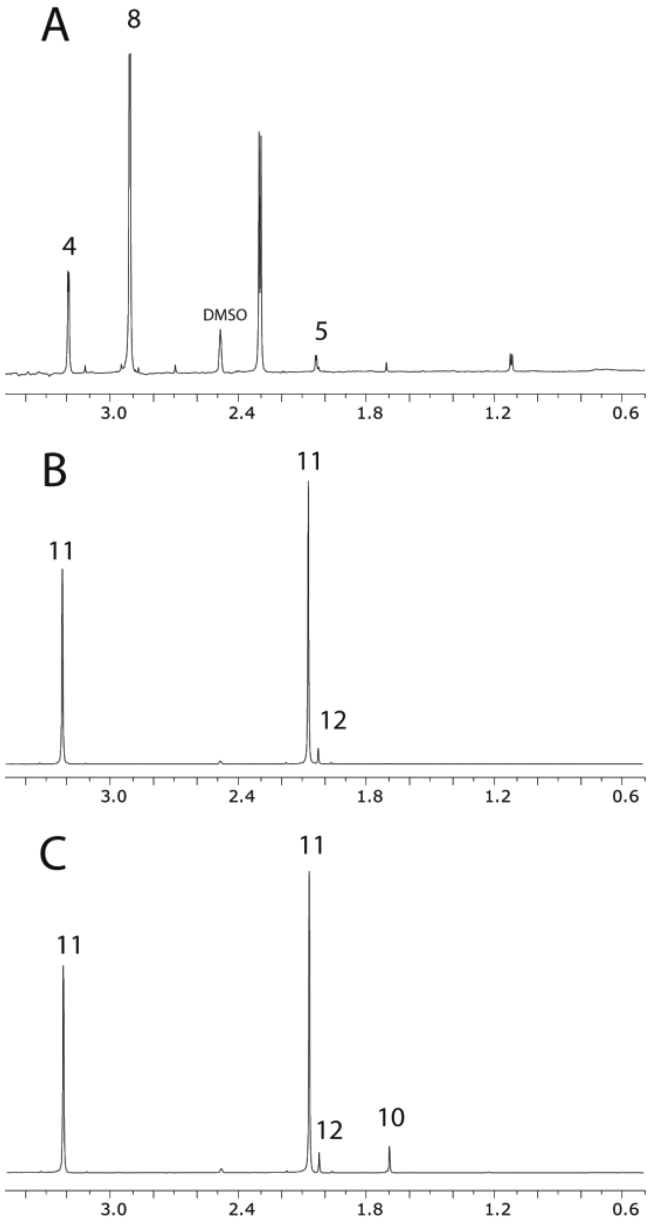

Figure 3. ^{1}H NMR spectroscopic product analysis of the reaction of E114D-Cg10062 with **8**, **9**, or **10**. (A) Products of E114D-Cg10062 with **8** (∼95 mM) after 3 min. (B) Products of E114D-Cg10062 with **9** (∼80 mM) after 3 min. (C) Products of E114D-Cg10062 with **10** (∼80 mM) after 3 min. All reactions contained ∼10.2 μM E114D-Cg10062 and 30 μL of DMSO-d_6. The reactions are individually scaled to show the product reaction. The scale can be assessed by the height of the DMSO peak, which is labeled in the spectra.

Kinetic Parameters of Y103F-Cg10062 with 2, 8, 9, and 10. The steady-state kinetic parameters for the reactions of **2**, **8**, **9**, and **10** with the Y103F mutant of Cg10062 are summarized in Table 4. With **8**, there was a 12-fold decrease in k_{cat} and a 6-fold decrease in K_m (vs wild type), resulting in a slight decrease in the k_{cat}/K_m. With **9**, the Y103F mutant of Cg10062 shows an 2-fold increase in the k_{cat}/K_m, which is due mostly to the 3.2-fold increase in k_{cat}. These observations parallel those made for the E114Q mutant of Cg10062. With **2**, there was a reduction in both k_{cat} and K_m (vs wild-type) resulting in a slightly higher k_{cat}/K_m value (∼4.3-fold) but lower than that for E114Q-Cg10062 (∼1.7-fold). With **10**, there was a significant increase (∼106-fold) in the value of k_{cat}/K_m. The Y103F mutant of Cg10062 showed very little activity with **3**, which precluded the measurement of kinetic parameters.

^{1}H NMR Characterization of the Y103F-Cg10062-catalyzed Reaction with 2, 3, 8, 9, and 10. The reactions of the Y103F mutant of Cg10062 with **2**, **3**, **8**, **9** and **10** were monitored by ^{1}H NMR spectroscopy (Figure 4). The results with **8** and the Y103F mutant are comparable to those observed for the wild type, although slower. Accordingly, the reaction of **8** with the Y103F mutant yields **4** (0.7%) and **5** (2.1%), along with unreacted substrate (97.2%) after 27 min (Figure 4A) (as indicated by the singlet at ∼2.9 ppm). The reaction of the Y103F mutant of Cg10062 with **2** yields **4** (1%) and **5** (8%) and unreacted substrate (91%) after 18 min (Figure 4B). The reaction with **3** is very slow, although a small signal for **4** (∼2.30 ppm) can be observed after 18 min (Figure 4C). The reaction of **9** with the Y103F mutant shows that **11** is the major product (99.5%) after 3 min (Figure 4D). A small amount of **12** (0.5%) is also present, which is slightly more than is expected for the nonenzymatic decarboxylation of **11**. The reaction of **10** with the Y103F mutant shows that the major product is **11** (84%), along with a significant amount of **12** (16%) after 6 min (Figure 4E). Hence, the Y103F mutant has hydratase/decarboxylase activity using **2**, **8**, and **10** as substrates. With **9**, it is mostly a hydratase.

Incubation of the E114D and Y103F Mutants of Cg10062 with 9 and 10 in the Presence of $NaCNBH_3$. Compounds **9** and **10** were incubated with the E114D and Y103F mutants overnight in the presence of $NaCNBH_3$, and the residual activity was determined using **9**. Three of the four mixtures had less than 10% remaining activity compared to the control (E114D and **9** or **10** and Y103F and **10**). The sample containing the Y103F mutant and **9** showed no loss in activity (vs the control). The ESI mass spectra of the three samples

Table 4. Steady-State Kinetic Parameters for the Y103F-Cg10062 Catalyzed Reactions[a]

	K_m (μM)	k_{cat} (s^{-1})	k_{cat}/K_m (M^{-1} s^{-1})
2	4700 ± 320	0.3 ± 0.04	60 ± 10
8	5 ± 1.8	0.5 ± 0.01	(1.0 ± 0.3) × 10^5
9	1150 ± 175	13 ± 2.5	(1.1 ± 0.3) × 10^4
10	650 ± 140	2.1 ± 0.2	(3.2 ± 0.8) × 10^3

[a]The kinetic parameters were measured by appropriate UV assay in 100 mM Na_2HPO_4 buffer (pH 8) at 22 °C.

DOI: 10.1021/acs.biochem.5b00240
Biochemistry 2015, 54, 3009−3023

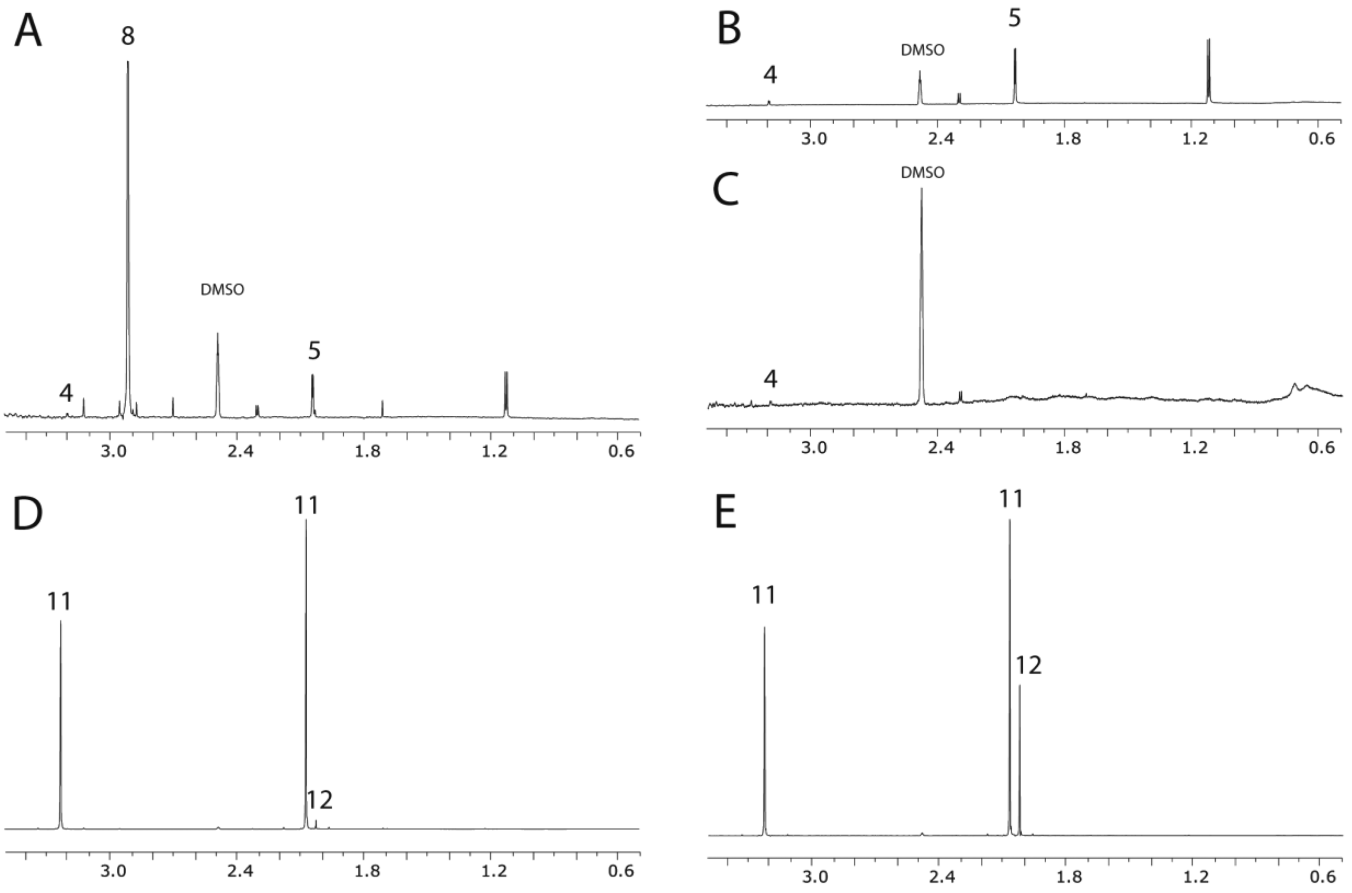

Figure 4. [1]H NMR spectroscopic product analysis of the reaction of Y103F-Cg10062 with **2**, **3**, **8**, **9**, or **10**. (A) Products of Y103F-Cg10062 with **8** (~95 mM) after 27 min. The reaction is not complete with **8** still present (~2.9 ppm). (B) Products of Y103F-Cg10062 with **2** (~63 mM) after 18 min. The reaction is not complete with **2** still present (NMR signals not shown). (C) The reaction of Y103F-Cg10062 with **3** (~63 mM) after 18 min. There are no observable signals for products except for a trace of **4** in the baseline. (D) Products of Y103F-Cg10062 with **9** (~80 mM) after 3 min. The small amount of **12** present is consistent with nonenzymatic decarboxylation of **11**. (E) Products of Y103F-Cg10062 with **10** (~80 mM) after 6 min. All reactions contained ~19.1 μM Y103F Cg10062 and 30 μL of DMSO-d_6. The reactions are individually scaled to show the product reaction. The scale can be assessed by the height of the DMSO peak, which is labeled in the spectra.

with reduced activities all showed two major signals: one at 17083−17085 Da and the other one at 17125−17126 Da (Figures 5A,B and 6).[1,21] The first signal corresponds to the expected mass for the unlabeled Cg10062 (calc, 17 085 Da), and the other signal corresponds to the mass of the covalently modified enzyme. The difference in mass is 42 Da, which is consistent with the mass of the reduced imine of acetone (**12**), one of the expected products of the reactions. In all three spectra, there is also a smaller signal at 17165−17168 Da. The difference in mass from that of control is 81−84 Da, which is consistent with the mass of the reduced imine of acetoacetate (**11**), the other expected product of these reactions. The range is within the instrumentation error, which is ±3 Da. (It is important to note that there is no loss in activity when the E114D or Y103F mutants are incubated with exogenous **11** or **12** in the presence of $NaCNBH_3$.) Because of the reactivity of the aldehyde products (i.e., **4** and **5**), trapping experiments were not carried out with Cg10062 and **8**.

Peptide Mapping and MALDI-MS Analysis. The location of the covalent modification was determined by proteolytic digestion using endoproteinase Glu-C (protease V-8), followed by MALDI-MS of the peptide fragments.[1,21] The spectra for the proteolytic digest of the E114D mutant with **9** or **10**, and the Y103F mutant with **10** are shown respectively in

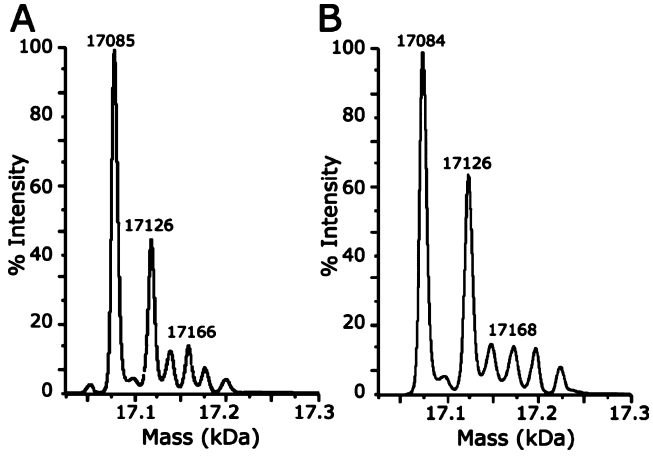

Figure 5. ESI-MS spectra of the E114D mutant of Cg10062 incubated with (A) **9** and (B) **10** in the presence of $NaCNBH_3$. The signals at 17 085 Da and 17 084 Da (in A and B, respectively) correspond to the unlabeled E114D-Cg10062. The signals at 17 126 Da correspond to E114D-Cg10062 covalently modified by the reduced imine of **12**. The smaller signals at 17 166 Da and 17 168 Da (in A and B, respectively) correspond to E114D-Cg10062 covalently modified by the reduced imine of **11**.

DOI: 10.1021/acs.biochem.5b00240
Biochemistry 2015, 54, 3009−3023

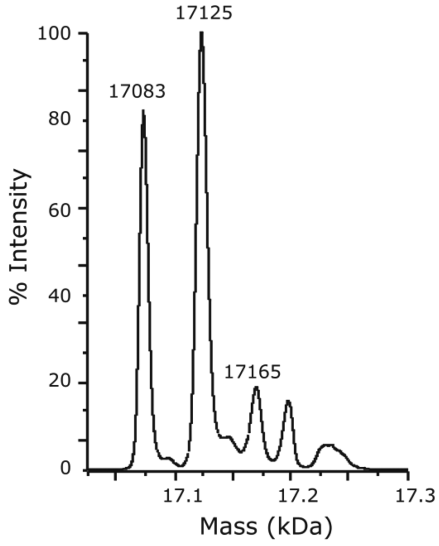

Figure 6. ESI-MS spectra of the Y103F mutant of Cg10062 incubated with **10** in the presence of $NaCNBH_3$. The signal at 17 083 Da corresponds to the unlabeled Y103F-Cg10062. The signals at 17 125 Da and 17 165 Da correspond to Y103F-Cg10062 covalently modified by the reduced imine of **12** and **11**, respectively.

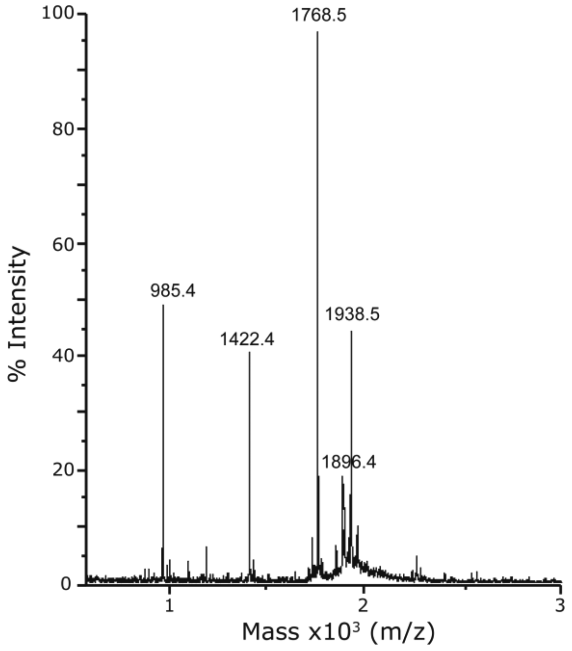

Figure 8. MALDI-MS of spectra of fragments from the proteolytic digest of the Y103F mutant of Cg10062 incubated with **10** and treated with $NaCNBH_3$. The signals for the five major peptide fragments are labeled and are assigned as follows: 985.4 Da, Leu-81 to Glu-88; 1422.4 Da, Tyr-115 to Glu-126; 1768.5 Da, Asn-61 to Glu-75; 1896.4 Da, Pro-1 to Glu-15; and 1938.5 Da, Pro-1 to Glu-15 (+42 Da). The mass difference of 42 Da on the Pro-1 to Glu-15 fragment is consistent with the covalent modification of the fragment by the reduced imine of **12**. Only the Pro-1 to Glu-15 fragment has a covalent adduct.

Figures 7A,B, and 8. All three spectra show a signal corresponding to the unmodified peptide Pro-1-Glu-15 (1896.2−1896.4 Da) as well as second signal corresponding to the same peptide modified by an adduct with a mass 42 Da (1938.3−1938.5 Da). This mass difference is consistent with the addition of the reduced imine of acetone (**12**) to the fragment. An examination of the sequence indicates that Pro-1 is the only chemically reasonable site for imine formation and subsequent covalent modification by reduction with $NaCNBH_3$. A signal for the reduced imine of acetoacetate (**11**) was not detected. The spectra show signals for additional peptide species in the samples (four major peptide fragments for the E114D mutant and three major peptide fragments for

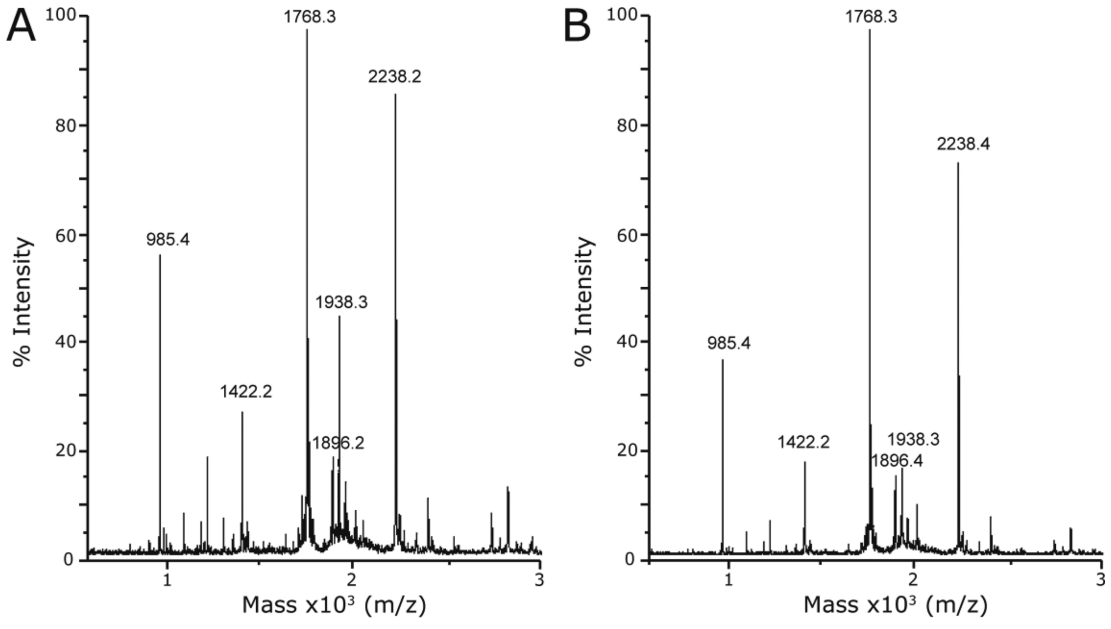

Figure 7. MALDI-MS of spectra of fragments from the proteolytic digest of the E114D mutant of Cg10062 incubated with (A) **9** and (B) **10** and treated with $NaCNBH_3$. The signals for the six major peptide fragments are labeled and are assigned as follows: 985.4 Da, Leu-81 to Glu-88; 1422.2 Da, Tyr-115 to Glu-126; 1768.3 Da, Asn-61 to Glu-75; 1896.2/1896.4 Da, Pro-1 to Glu-15; 1938.3 Da, Pro-1 to Glu-15 (+ 42 Da); and 2238.2/2238.4 Da, Ile-107 to Glu-126. The mass difference of 42 Da on the Pro-1 to Glu-15 fragment is consistent with the covalent modification of the fragment by the reduced imine of **12**. Only the Pro-1 to Glu-15 fragment has a covalent adduct.

DOI: 10.1021/acs.biochem.5b00240
Biochemistry 2015, 54, 3009−3023

the Y103F mutant). However, none of these peptide fragments is modified by a covalent adduct.

Protease V-8 hydrolyzes peptides at the carboxylate side of glutamate and aspartate residues with a preference for the glutamyl residues.[22,23] Proteolysis is dependent on the buffer conditions as well as the residues adjacent to the site of hydrolysis. Interestingly, the E114D mutant shows a slightly different pattern than that for the Y103F mutant. The protease does not hydrolyze the protein at Asp-114 in the E114D mutant but does hydrolyze at Glu-114 in the Y103F mutant. This observation provides additional confirmation for the identities of two enzymes.

DISCUSSION

The mechanism of *cis*-CaaD has been studied extensively,[3,11,12,21,24−27] and the results of these studies provide the context for the reactions of Cg10062 with **8**, **9**, and **10**. Sequence analysis first linked *cis*-CaaD to the tautomerase superfamily and identified four of the six residues (Pro-1, Arg-70, Arg-73, and Glu-114) now known to be required for activity.[3] Mutagenesis showed that three of these residues are critical for *cis*-CaaD activity: the P1A, R70A, and R73A mutants of *cis*-CaaD lacked any detectable activity. However, the E114Q mutant retained some activity (8-fold reduction in k_{cat}/K_m using **2**), which hinted that an additional residue(s) might be involved in the activation of a water molecule (later identified at Tyr-103). This initial characterization also showed that *cis*-CaaD catalyzed the hydration of the acetylene compound **6** to produce **7** with a 582-fold reduction in k_{cat}/K_m (compared with that measured for the CaaD-catalyzed reaction).

Analysis of a crystal structure of *cis*-CaaD covalently modified at Pro-1 by (*R*)-2-hydroxypropanoate (**14**, Scheme 5) identified a second water-activating residue (Tyr-103) and a sixth residue (His-28).[24,25] Covalent modification resulted from the incubation of *cis*-CaaD with the (*R*)-isomer of oxirane-2-carboxylate (**13**).[24] Mutagenesis confirmed the importance of these two residues for *cis*-CaaD activity. The structure also suggested how substrate might bind in the active site (Scheme 6).

In the course of this study, a pH rate profile of the wild-type reaction identified a protonated group with a pK_a of ∼9.3 that is required for activity.[24] The group is proposed to be Pro-1, which is consistent with the observed hydration of **6** to **7** involving a cationic Pro-1.[4]

On the basis of all of these observations, the mechanism shown in Scheme 6 was formulated for *cis*-CaaD (using **2**). In this mechanism, the carboxylate group interacts with the three positively charged residues (Arg-70, Arg-73, and His-28).[25,27] The interactions serve to bind and polarize the substrate. Polarization of the substrate generates a partial positive charge at C-3 and sets up the substrate for a Michael addition of water. Glu-114 and Tyr-103 activate the water molecule for attack at C-3 to produce the *aci*-carboxylate species **15**. This species undergoes one of the two fates shown in paths A and B. In path A, Pro-1 provides a proton at C-2 to produce **16**. Expulsion of HCl from **16** affords **4**. In path B, **15** undergoes an α,β-elimination reaction to produce **17**. Tautomerization of **17** yields **4**.

Scheme 5. Irreversible Inactivation of *cis*-CaaD by (*R*)-Oxirane-2-carboxylate (13)

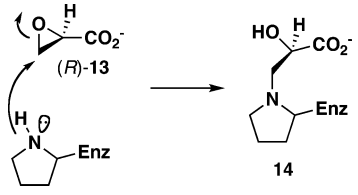

In addition to **6**, compounds **8**, **9**, and **10** were examined as substrates for *cis*-CaaD. Both compounds are reasonably good substrates for *cis*-CaaD with k_{cat}/K_m values of 6.4×10^3 M^{-1} s^{-1} (**8**)[28] and 8.7×10^3 M^{-1} s^{-1} (**9**).[11,21] Compound **10** is not processed to any appreciable extent.[28] For both of the substrates, the hydration product (**4** or **11**, respectively) is not decarboxylated by the enzyme.

It was anticipated that *cis*-CaaD would catalyze the direct addition of water to C-3 of both compounds, paralleling the reaction mechanism for the enzyme with **6** (Scheme 2A). However, in the presence of **9** and $NaCNBH_4$, *cis*-CaaD was irreversibly inactivated by the covalent modification of the prolyl nitrogen of Pro-1.[21] Subsequent study including a detailed kinetic analysis showed that the hydration of **9** occurs by covalent catalysis where Pro-1 forms an enamine with **9**.[21] Hydrolysis of the enamine or the imine tautomer produces **4**. This is the first example of covalent catalysis in the tautomerase superfamily.

A database search for *cis*-CaaD family members identified Cg10062.[1] The conserved six active site residues, the sequence similarity, and the nearly identical active site region suggested that the activity and mechanism would be comparable to those of *cis*-CaaD, even though the genomic context did not show the presence of any enzymes in the 1,3-dichloropropene catabolic pathway or homologues of these enzymes.[1] Characterization of Cg10062 showed that this assumption was not correct.

Our studies uncovered three striking differences. First, Cg10062 is a poor dehalogenase using **2** and is a nonspecific dehalogenase in that it will process **3** (although poorly).[1] Second, the enzyme is inactivated by both isomers of **13**, with the (*R*)-isomer being more potent.[2] This observation parallels the enzyme's ability to process both **2** and **3**. Finally, Cg10062 catalyzes the direct addition of water to the allene (**9**), whereas *cis*-CaaD uses covalent catalysis to hydrate the compound. A stereochemical analysis of the two enzymes (using **9**) shows that they incorporate a deuteron on opposite faces. The different stereochemical consequences could be a result of the different mechanisms, binding modes, proton sources, or some combination of the three.[21]

Frequently, two closely related enzymes do not have comparable levels of activity using the same substrate(s) or even the same activities.[29−31] This observation can be due to subtle changes in the active site that alter the positions of catalytic and/or binding residues. It can also result from elements outside the active site where the sequence similarities are not as high.[30,31] These elements might include a mobile loop or conformational dynamics.[11,30,31] Finally, the two enzymes might have different substrates or entirely different activities. The work presented here shows that Cg10062 has a different activity than *cis*-CaaD using the same substrate.

The reaction of *cis*-CaaD and **8** produces only **4**. In contrast, the reaction of **8** and Cg10062 produces a small amount of **4** (25%) and mostly **5** (75%). Hence, Cg10062 functions as a hydratase/decarboxylase, whereas *cis*-CaaD functions as a hydratase. The unique feature of the Cg10062-catalyzed reaction is that the decarboxylation reaction *depends* on the hydration reaction. In other words, Cg10062 does not catalyze

DOI: 10.1021/acs.biochem.5b00240
Biochemistry 2015, 54, 3009−3023

Scheme 6. Catalytic Mechanism for *cis*-CaaD

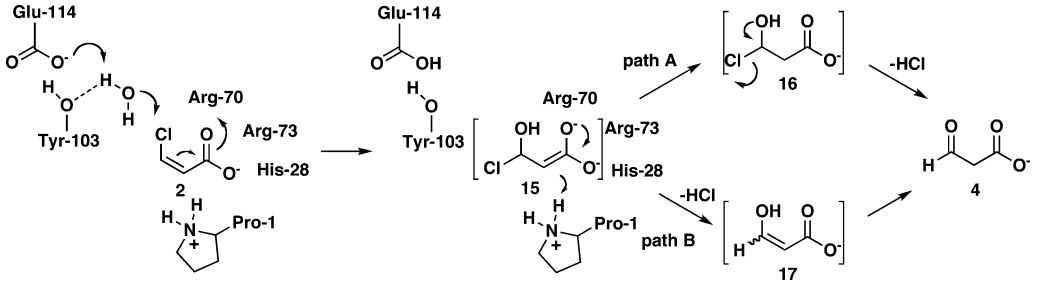

the decarboxylation of **4** when added exogenously. It is known that the exogenously added **4** binds at the active site with a K_d of about 25 mM (J. P. Huddleston, W. H. Johnson, Jr., and C. P. Whitman, unpublished results, 2015). Moreover, although **4** is a reasonable intermediate in the transformation of **8** to **5**, it might not be generated as a discrete intermediate. Understanding how Cg10062 catalyzes the decarboxylation reaction of this hydration-dependent reaction is critical for elucidating the enzyme's mechanism.

Several mechanisms have been reported for the decarboxylation of β-keto acids.[32−34] For a start, the hydration-dependent decarboxylation reaction reported here is coenzyme and metal ion independent (as is the hydration reaction), eliminating mechanisms that require a cofactor. Cofactor-independent β-ketoacid decarboxylases have been described that use a Schiff base mechanism (e.g., acetoacetate decarboxylase[32]) or an oxyanion hole (e.g., MSAD[10,20,33] and methylmalonyl CoA decarboxylase[34]). For Cg10062, the Schiff base would form between Pro-1 and substrate. These mechanisms might not be directly applicable to Cg10062 because the decarboxylation reaction is entirely dependent on the hydration reaction. This suggests that Cg10062 might proceed by an unprecedented mechanism. In view of these considerations, three mechanisms can be envisioned for the hydratase/decarboxylase activity of Cg10062 where the interaction of the substrate carboxylate group with Arg-70, Arg-73, and His-28 most likely positions it in the active site. The first mechanism involves the Cg10062-catalyzed hydration of **8** to produce **4**, followed by the decarboxylation of **4** to yield **5** (Scheme 7). Water is activated by the combination of Glu-114 and Tyr-103, and the molecule is polarized by the combination of Arg-70, Arg-73, and His-28 (analogous to the roles assigned to these residues in Scheme 6). This results in **17**, which can tautomerize to **4**. Pro-1 (with an assumed pK_a value of 9.2 based on the pH rate profile for *cis*-CaaD) provides the proton at C-2 in the initial hydration step (to form **17**) or in the tautomerization step. An amount of **4** (~25%) is released from the active site, and the remaining **4** is decarboxylated by an unknown mechanism. An analogous mechanism can be envisioned for the hydration/decarboxylation of **2**.

This mechanism is at odds with the observation that exogenously added **4** is not decarboxylated by the enzyme and argues against it. However, if this mechanism is operative, one could argue that the hydration of **8** positions **4** in an orientation for decarboxylation. The positioning of **4** in the active site appears to be an important factor for its decarboxylation. The hydration of **3** also produces **4**, but **4** is not decarboxylated. Hence, the hydration of **8** (and **2**) could place **4** in a favorable state for decarboxylation, which is not achieved by the hydration of **3** or by exogenously added **4**. Another possibility is that **4** is not generated as a distinct entity in the hydration-dependent decarboxylation of **8** (and **2**).

In a second mechanism, the hydration step is followed by the formation of a covalent intermediate between Pro-1 (now nucleophilic because the proton was removed in the hydration step) and C-3 of **4** (i.e., a Schiff base) (Scheme 8). The reactivity of the aldehyde could facilitate the process. Decarboxylation of the Schiff base (**18**) generates the enamine, **19**, which can tautomerize to **20**. Hydrolysis of **20** generates **5** and free enzyme. A small amount of **4** could escape from the active site and not form a Schiff base (accounting for the 25% of **4** in the final mixture). In this mechanism, the exogenously added **4** might not be decarboxylated because Pro-1 is not in the correct protonation state to form the Schiff base intermediate. The hydration reaction necessarily occurs first in order to put Pro-1 into the correct state. The same sequence of events could process **2**.

The third mechanism involves covalent catalysis using Pro-1 (Scheme 9). Accordingly, Pro-1 adds to C-3 of **8** to form **21**, which can rearrange to **18**. The occasional hydrolysis of **18**

Scheme 7. Cg10062-Catalyzed Hydration of 8 by Direct Attack of Water Followed by Decarboxylation

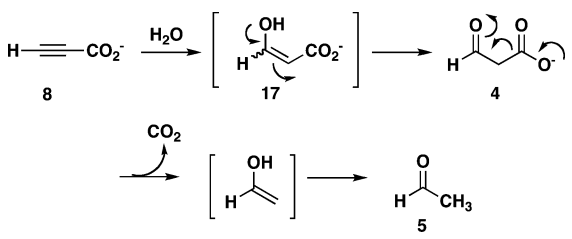

Scheme 8. Cg10062-Catalyzed Hydration of 8 by Direct Attack of Water Followed by Decarboxylation via a Schiff Base

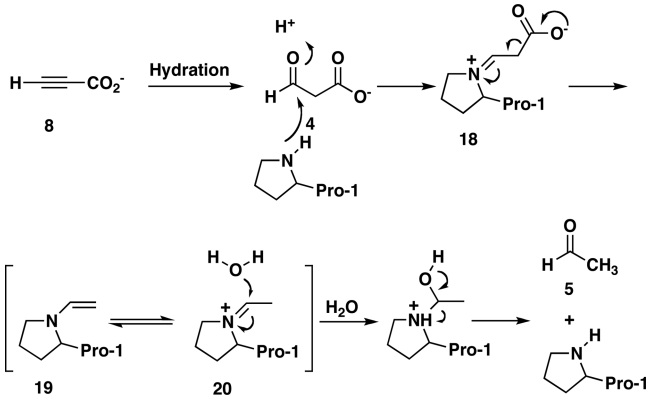

DOI: 10.1021/acs.biochem.5b00240
Biochemistry 2015, 54, 3009−3023

Scheme 9. Cg10062-Catalyzed Hydration of 8 by a Covalent Catalysis Mechanism

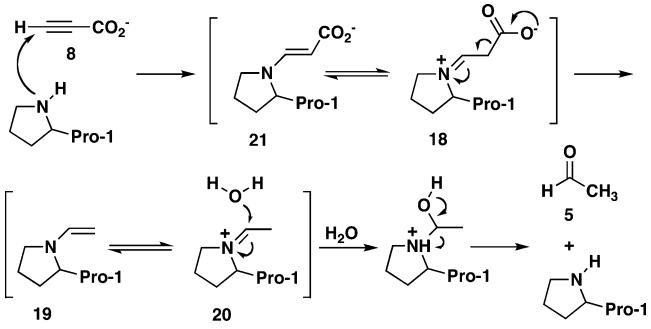

produces the small amount of **4**. Otherwise, the decarboxylation of **18** forms **19**, which tautomerizes to **20**. Hydrolysis of **20** yields **5** and free enzyme. An analogous mechanism is not likely for **2**.

One potential drawback to this third mechanism is that the apparent pK_a of Pro-1 (~9.2), inferred again from the pH rate profile of *cis*-CaaD, suggests that the prolyl nitrogen is largely cationic and unable to function as a nucleophile. If this mechanism is operative, there could be two explanations for this discrepancy: the pH rate profile does not reflect the actual pK_a of the prolyl nitrogen in Cg10062 or the reaction proceeds using the small amount of enzyme with the prolyl nitrogen in the uncharged form. (For the third mechanism, the small amount of enzyme in the uncharged form would readily react with the aldehyde moiety of exogenously added **4** and result in decarboxylation. This does not happen. A satisfactory explanation is not apparent.)

It is unknown how Cg10062 catalyzes the decarboxylation reaction in the hydration-dependent decarboxylation sequence in the first mechanism (Scheme 7). The Schiff base in the second and third mechanisms (Schemes 8 and 9) lends itself to decarboxylation (although it is not known which residues and other features of the active site are involved). Obviously, delineating the decarboxylation mechanism would narrow the mechanistic possibilities.

The reactions of **9** and **10** with Cg10062 produce only the hydration product (**11** for both substrates). Hence, for these substrates, Cg10062 functions as a hydratase. The most obvious difference between **8** and these substrates is length (3 vs 4 carbons). These observations could suggest that the positioning of substrate in the active site plays an important role in the outcome (hydration vs hydration/decarboxylation). In addition, the hydration product, **11**, is a ketone with an extra methyl group (vs **4**). These features could further contribute to the reaction outcome. However, there still remains any number of explanations without knowing how Cg10062 catalyzes the decarboxylation part of the hydration-dependent decarboxylation of **8**.

In an effort to understand the Cg10062 reaction mechanism, the two water-activating residues (Glu-114 and Tyr-103) were examined by mutagenesis, and their reactions with **8**, **9**, and **10** were characterized (Table 5, Figure 9). This analysis produced a range of results, which are mostly perplexing and not obviously explained. The easier results to rationalize are those that involve a reduction in wild type activity (e.g., Y103F with **8**). In these cases, the mutation could disrupt binding, the catalytic machinery, or both, to produce a less efficient enzyme.

It is more difficult to explain the switch in activities where the hydratase/decarboxylases lose decarboxylase activity or the hydratases gain decarboxylase activity. With **2** and **8**, the E114 mutants (E114Q and E114D) lose decarboxylase activity and function only as hydratases. With **2**, the E114D mutant is a poor hydratase, whereas with **8**, it has more significant activity. This is based on the ^{1}H NMR analysis, which shows that the mutant generates product at a faster rate using **8**. The same analysis shows that the E114Q mutant is a better hydratase with **2** than it is with **8** (but not as effective as the E114D mutant with **10**). The other switch in activity is the gain of function. With **9** and **10**, the E114Q mutant functions as a hydratase/decarboxylase as does the Y103F mutant with **10**. ^{1}H NMR analysis also suggests that the Y103F mutant (with **10**) and the E114Q mutant (with **9**) have significant hydratase/decarboxylase activity (but not comparable to the hydratase/decarboxylase activity of the wild type with **8**). Several factors could be responsible for the gain of function ranging from a longer time in the active site to a more roomy, less constrained active site resulting in accessibility to C-3 of the substrate. Again, understanding how Cg10062 and the mutants catalyze the decarboxylation part of the hydration-dependent decarboxylation of **8** shortens the list of possibilities. Efforts are underway to do this.

For two of the mutant enzymes (E114D and Y103F), it was possible to trap the equivalent of the hydration product (**11** from **9** or **10** processed by E114D and **11** from **10** processed by the Y103F mutant) and the decarboxylation product (**12**) as the reduced imine covalently attached to Pro-1 (using $NaCNBH_3$). It is not possible to trap the reduced imine by incubating the two mutants with exogenously added **11** or **12**. This result is tantalizing and seems to suggest that covalent catalysis is operative (Schemes 8 or 9). However, there are concerns. First, it is not possible to trap any imine when the same experiment is carried out with the E114Q mutant and **9**. This enzyme has a pronounced hydratase/decarboxylase activity (after 12 min, the mixture consists of 83% of **11** and 17% of **12**). Second, it is not clear why the imine of **12** is trapped when the E114D mutant is incubated with **9** and **10** because **12** is not present in very large amounts (~2.5%).

Table 5. Summary of the Activities for Cg10062 and Mutants

substrate	wild type	Y103F	E114Q	E114D
2	hydratase/decarboxylase	hydratase/decarboxylase	hydratase	hydratase
3	hydratase	ND[a]	ND[a]	ND[a]
8	hydratase/decarboxylase	hydratase/decarboxylase	hydratase	hydratase
9	hydratase	hydratase	hydratase/decarboxylase	hydratase[b]
10	hydratase[b]	hydratase/decarboxylase	hydratase/decarboxylase	hydratase[b]

[a]Activity is not detected by UV or ^{1}H NMR spectroscopy. [b]Trace amounts of **12** (~0.3−2.8%) are present in the ^{1}H NMR spectra, but these enzymes function primarily as hydratases. Assay conditions are described in the text.

DOI: 10.1021/acs.biochem.5b00240
Biochemistry 2015, 54, 3009−3023

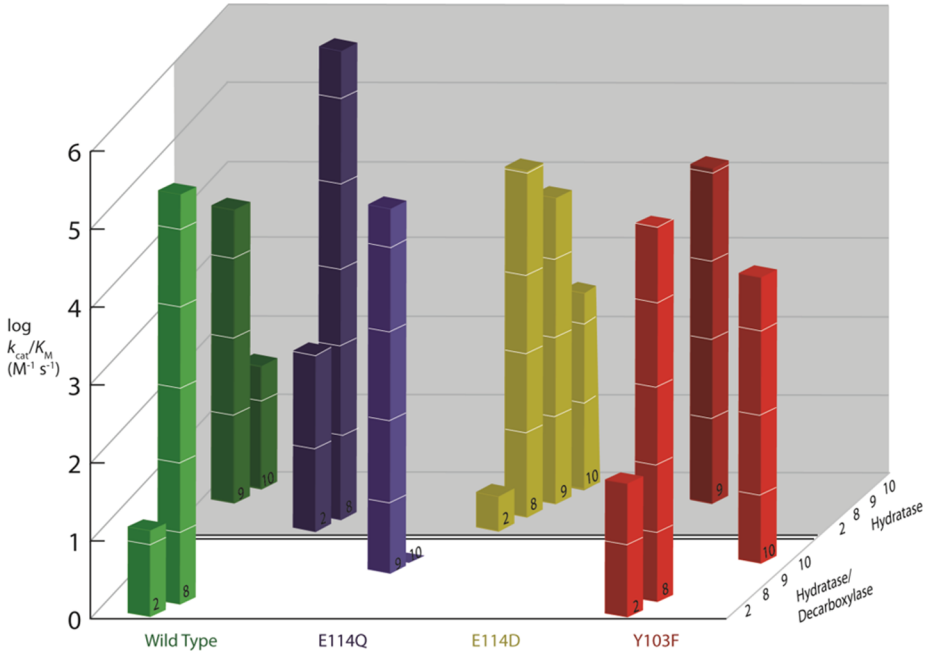

Figure 9. Bar graph showing the activities for wild type Cg10062 and the E114Q-, E114D-, and Y103F mutants of Cg10062 with **2**, **8**, **9**, and **10**. The activities for the four substrates (**2**, **8**, **9**, and **10**) with Cg10062, and with the E114Q-, E114D-, and Y103F mutants of Cg10062 are shown in the green, blue, yellow, and red bars, respectively. The set of bars in the forefront (lighter shades of these colors) represents enzyme and substrate combinations showing hydratase/decarboxylase activity. The set of bars in the background (darker shades) represents enzyme and substrate combinations showing only hydratase activity. The height of each bar indicates the log (k_{cat}/K_m) values (in M^{-1} s^{-1}) for the four substrates.

These observations raise the possibility that the trapping results are experimental artifacts (e.g., the $NaCNBH_3$ might alter the course of the reaction).

Although **8** is clearly the "best" substrate identified for Cg10062 thus far (as suggested by the high k_{cat}/K_m of 1.8×10^5 M^{-1} s^{-1}), the biological relevance of the hydratase/decarboxylase activity with this substrate is not clear. Acetylene-bearing natural products are well-known (e.g., the enediyne antibiotics), and there are various reports about the bacterial catabolism of acetylenes, but not in *C. glutamicum*.[35−37] The genomic context for Cg10062 is not informative because the adjacent genes have unknown functions or annotated functions that are not useful.[1] There are, however, two reports about the bacterial transformation of **8** that could have implications for the biological relevance. First, a strain of *Pseudomonas putida* that was isolated from rotting fruit was shown to use **8** as a sole carbon source.[36] ^1H NMR spectroscopy following the transformation of **8** in these *P. putida* cells showed the transformation of **8** to **4** and **5**. However, the enzyme(s) responsible for this transformation and whether the conversion of **4** to **5** is an enzyme-catalyzed reaction (or not) were not reported. The identification of the enzyme responsible for this transformation and any genomic context could shed light on the role of Cg10062. A second report in the KEGG database outlines a pathway for the conversion of **8** to **4**, followed by the conversion of **4** to *β*-alanine.[37] The basis for this series of conversions is not entirely clear, but *β*-alanine can be processed to pantothenic acid in *C. glutamicum*, which is known for the overproduction of pantothenic acid. (*β*-alanine can be routed to other pathways as well.[38]) This pathway does not account for the production of **5** in any obvious way, and the connection between Cg10062 and the pathway is tenuous at best, but it is an intriguing possibility. Bioinformatics approaches (e.g., sequence similarity and genomic neighborhood networks) are currently being applied to the tautomerase superfamily and may ultimately uncover the physiological relevance of the hydratase/decarboxylase activity.[39]

Finally, the hydratase/decarboxylase activity of wild type Cg10062 with the *cis*-3-haloacrylates has an intriguing evolutionary implication. The isomer-specific dehalogeneases (*cis*-CaaD and CaaD) and MSAD are all tautomerase superfamily members that are found in the 1,3-dichloropropene catabolic pathway, where they catalyze successive reactions (Scheme 1).[4,6,7] *cis*-CaaD and MSAD have additional similarities: both are homotrimers with comparably sized monomers (129 amino acids for MSAD and 149 amino acids for *cis*-CaaD),[25,27,33] and both catalyze the hydration of **6** to yield **7** (Scheme 2).[3,10,13] For these reasons, the dehalogenases and MSAD might have diverged from a common ancestral enzyme that catalyzed both reactions.[1] Although Cg10062 might not be the progenitor, it might be representative of the progenitor. The bioinformatics approaches described above could provide more clues.[39]

AUTHOR INFORMATION

Corresponding Author

*Tel (512) 471-6198. Fax (512) 232-2606. E-mail whitman@austin.utexas.edu.

Funding

This research was supported by the National Institutes of Health Grant GM-65324 (C.P.W.), a fellowship award (F32 GM089083) from the National Institute of General Medical Sciences to G.K.S., and the Robert A. Welch Foundation (F-1334).

Notes

The authors declare no competing financial interest.

DOI: 10.1021/acs.biochem.5b00240
Biochemistry 2015, 54, 3009−3023

■ ACKNOWLEDGMENTS

The protein mass spectrometry analysis was conducted in the Institute for Cellular and Molecular Biology Protein and Metabolite Analysis Facility at the University of Texas at Austin. We thank Steve D. Sorey (Department of Chemistry, University of Texas at Austin) for his expert assistance in the acquisition of the ^{1}H NMR spectra.

■ ABBREVIATIONS

Ap, ampicillin; CaaD and *cis*-CaaD, *trans*- and *cis*-3-chloroacrylic acid dehalogenase, respectively; DMSO, dimethyl sulfoxide; ESI-MS, electrospray ionization-mass spectrometry; LB, Luria−Bertani; MALDI-MS, matrix-assisted laser desorption/ionization-mass spectrometry; MSAD, malonate semialdehyde decarboxylase; NMR, nuclear magnetic resonance; PCR, polymerase chain reaction; SDS-PAGE, sodium dodecyl sulfate-polyacrylamide gel electrophoresis

■ REFERENCES

(1) Poelarends, G. J., Serrano, H., Person, M. D., Johnson, W. H., Jr, and Whitman, C. P. (2008) Characterization of Cg10062 from *Corynebacterium glutamicum*: Implications for the evolution of *cis*-3-chloroacrylic acid dehalogenase activity in the tautomerase superfamily. *Biochemistry 47*, 8139−8147.

(2) Robertson, B. A., Johnson, W. H., Jr., Lo, H. H., and Whitman, C. P. (2008) Inactivation of Cg10062, a *cis*-3-chloroacrylic acid dehalogenase homologue in *Corynebacterium glutamicum*, by (*R*)- and (*S*)-oxirane-2-carboxylate: analysis and implications. *Biochemistry 47*, 8796−8803.

(3) Poelarends, G. J., Serrano, H., Person, M. D., Johnson, W. H., Jr., Murzin, A. G., and Whitman, C. P. (2004) Cloning, expression, and characterization of a *cis*-3-chloroacrylic acid dehalogenase: Insights into the mechanistic, structural, and evolutionary relationship between isomer-specific 3-chloroacrylic acid dehalogenases. *Biochemistry 43*, 759−772.

(4) Poelarends, G. J., Veetil, V. P., and Whitman, C. P. (2008) The chemical versatility of the *β*-*α*-*β* fold: catalytic promiscuity and divergent evolution in the tautomerase superfamily. *Cell. Mol. Life Sci. 65*, 3606−3618.

(5) Murzin, A. G. (1996) Structural classification of proteins: New superfamilies. *Curr. Opin. Struct. Biol. 6*, 386−394.

(6) Poelarends, G. J., Wilkens, M., Larkin, M. J., Van Elsas, J. D., and Janssen, D. B. (1998) Degradation of 1,3-dichloropropene by *Pseudomonas cichorii* 170. *Appl. Environ. Microbiol. 64*, 2931−2936.

(7) Van Hylckama Vlieg, J. E. T., and Janssen, D. B. (1992) Bacterial degradation of 3-chloroacrylic acid and the characterization of *cis*- and *trans*-specific dehalogenases. *Biodegradation 2*, 139−150.

(8) Hartmans, S., Jansen, M. W., Van der Werf, M. J., and De Bont, J. A. M. (1991) Bacterial metabolism of 3-chloroacrylic acid. *J. Gen. Microbiol. 137*, 2025−2032.

(9) Poelarends, G. J., Saunier, R., and Janssen, D. B. (2001) *trans*-3-Chloroacrylic acid dehalogenase from *Pseudomonas pavonaceae 170* shares structural and mechanistic similarities with 4-oxalocrotonate tautomerase. *J. Bacteriol. 183*, 4269−4277.

(10) Poelarends, G. J., Johnson, W. H., Jr., Murzin, A. G., and Whitman, C. P. (2003) Mechanistic characterization of a bacterial malonate semialdehyde decarboxylase: identification of a new activity on the tautomerase superfamily. *J. Biol. Chem. 278*, 48674−48683.

(11) Schroeder, G. K., Huddleston, J. P., Johnson, W. H., Jr., and Whitman, C. P. (2013) A mutational analysis of the active site loop residues in *cis*-3-chloroacrylic acid dehalogenase. *Biochemistry 52*, 4204−4216.

(12) Robertson, B. A., Schroeder, G. K., Jin, Z., Johnson, K. A., and Whitman, C. P. (2009) Pre-steady-state kinetic analysis of *cis*-3-chloroacrylic acid dehalogenase: Analysis and implications. *Biochemistry 48*, 11737−11744.

(13) Wang, S. C., Person, M. D., Johnson, W. H., Jr., and Whitman, C. P. (2003) Reactions of *trans*-3-chloroacrylic acid dehalogenase with acetylene substrates: consequences of and evidence for a hydration reaction. *Biochemistry 42*, 8762−8773.

(14) Eglinton, G., Jones, E. R. H., Mansfield, G. H., and Whiting, M. C. (1954) Acetylenic compounds. XLV. The alkaline isomerization of but-3-ynoic acid. *J. Chem. Soc.*, 3197−3200.

(15) Sambrook, J., Fritsch, E. F., and Maniatis, T. (1989) *Molecular Cloning: A Laboratory Manual*, 2nd ed., Cold Spring Harbor Laboratory, Cold Spring Harbor, NY.

(16) Waddell, W. J. (1956) A simple ultraviolet spectrophotometric method for the determination of protein. *J. Lab. Clin. Med. 48*, 311−314.

(17) Laemmli, U. K. (1970) Cleavage of structural proteins during the assembly of the head of bacteriophage T4. *Nature 227*, 680−685.

(18) Serrano, H. (2009) Characterization of the activities of *trans*-3-chloroacrylic acid dehalogenase and *cis*-3-chloroacrylic acid dehalogenase and malonate semialdehyde decarboxylase homologues: Mechanism and evolutionary implications. Ph. D. Thesis. University of Texas at Austin.

(19) Johnson, K. A. (1992) Transient-state kinetic analysis of enzyme reaction pathways. In *The Enzymes* (Sigman, D. S., Ed.) 3rd ed, pp 1−61, Academic Press, San Diego.

(20) Guo, Y., Serrano, H., Poelarends, G. J., Johnson, W. H., Jr., Hackert, M. L., and Whitman, C. P. (2013) Kinetic, mutational, and structural analysis of malonate semialdehyde decarboxylase from *Coryneform* bacterium strain FG41: mechanistic implications for the decarboxylase and hydratase activities. *Biochemistry 52*, 4830−4831.

(21) Schroeder, G. K., Johnson, W. H., Jr., Huddleston, J. P., Serrano, H., Johnson, K. A., and Whitman, C. P. (2012) Reaction of *cis*-3-chloroacrylic acid dehalogenase with an allene substrate, 2,3-butadienoate: hydration via an enamine. *J. Am. Chem. Soc. 134*, 293−304.

(22) Houmard, J., and Drapeau, G. R. (1972) Staphylococcal protease: a proteolytic enzyme specific for glutamoyl bonds. *Proc. Natl. Acad. Sci. U.S.A. 69*, 3506−3509.

(23) Sorensen, S. B., Sørenson, T. L., and Breddam, K. (1991) Fragmentation of proteins by *S. aureus* strain V8 protease. Ammonium bicarbonate strongly inhibits the enzyme but does not improve the selectivity for glutamic acid. *FEBS Lett. 294*, 195−197.

(24) Poelarends, G. J., Serrano, H., Johnson, W. H., Jr., and Whitman, C. P. (2004) Stereospecific alkylation of *cis*-3-chloroacrylic acid dehalogenase by (*R*)-oxirane-2-carboxylate: analysis and mechanistic implications. *Biochemistry 43*, 7187−7196.

(25) de Jong, R. M., Bazzacco, P., Poelarends, G. J., Johnson, W. H., Jr, Kim, Y.-J., Burks, E. A., Serrano, H., Thunnissen, A.-M.W.H., Whitman, C. P., and Dijkstra, B. W. (2007) Crystal structures of native and inactivated *cis*-3-chloroacrylic acid dehalogenase: structural basis for substrate specificity and inactivation by (*R*)-oxirane-2-carboxylate. *J. Biol. Chem. 282*, 2440−2449.

(26) Sevastik, R., Whitman, C. P., and Himo, F. (2009) Reaction mechanism of *cis*-3-chloroacrylic acid dehalogenase - a theoretical study. *Biochemistry 48*, 9641−9649.

(27) Guo, Y., Serrano, H., Johnson, W. H., Jr., Ernst, S., Hackert, M. L., and Whitman, C. P. (2011) Crystal structures of native and inactivated *cis*-3-chloroacrylic acid dehalogenase: implications for the catalytic and inactivation mechanisms. *Bioorg. Chem. 39*, 1−9.

(28) Huddleston, J. P., Johnson, W. H., Jr., Schroeder, G. K., and Whitman, C. P. (2015) The accidental assignment of function in the tautomerase superfamily. *Perspect. Sci. 4*, 38−45.

(29) Lu, Z., Dunaway-Mariano, D., and Allen, K. N. (2011) The X-ray crystallographic structure and specificity profile of HAD superfamily phosphohydrolase BT1666: comparison of paralogous functions in *B. thetaiotaomicron*. *Proteins 79*, 3099−3107.

(30) Li, L., Luo, M., Ghanem, M., Taylor, E. A., and Schramm, V. L. (2008) Second-sphere amino acids contribute to transition-state structure in bovine purine nucleoside phosphorylase. *Biochemistry 47*, 2577−2583.

DOI: 10.1021/acs.biochem.5b00240
Biochemistry 2015, 54, 3009−3023

(31) Whittier, S. K., Hengge, A. C., and Loria, J. P. (2013) Conformational motions regulate phosphoryl transfer in related protein tyrosine phosphatases. *Science 341*, 899−903.
(32) Ho, M. C., Menetret, J. F., Tsuruta, H., and Allen, K. N. (2009) The origin of the electrostatic perturbation in acetoacetate decarboxylase. *Nature 459*, 393−397.
(33) Almrud, J. J., Poelarends, G. J., Johnson, W. H., Jr., Serrano, H., Hackert, M. L., and Whitman, C. P. (2005) Crystal structures of the wild-type, P1A mutant, and inactivated malonate semialdehyde decarboxylase: a structural basis for the decarboxylase and hydratase activities. *Biochemistry 44*, 14818−14827.
(34) Benning, M. M., Haller, T., Gerlt, J. A., and Holden, H. M. (2000) New reactions in the crotonase superfamily: Structure of methylmalonyl CoA decarboxylase from *Escherichia coli*. *Biochemistry 39*, 4630−4639.
(35) Yamada, E. W., and Jakoby, W. B. (1958) Enzymatic utilization of acetylenic compounds. II. Acetylenemonocarboxylic acid hydrase. *J. Biol. Chem. 233*, 941−945.
(36) Brecker, L., Petschnigg, J., Depine, N., Weber, H., and Ribbons, D. W. (2003) *In situ* proton NMR analysis of α-alkynoate biotransformations: from 'invisible substrates' to detectable metabolites. *Eur. J. Biochem. 270*, 1393−1398.
(37) Kanehisa, M., Goto, S., Kawashima, S., and Nakaya, A. (2002) The KEGG databases at GenomeNet. *Nucleic Acids Res. 30*, 42−46.
(38) Merkamm, M., Chassagnole, C., Lindley, N. D., and Guyonvarch, A. (2003) Ketopantoate reductase activity is only encoded by *ilvC* in *Corynebacterium glutamicum*. *J. Biotechnol. 104*, 253−260.
(39) Zhao, S., Sakai, A., Zhang, X., Vetting, M. W., Kumar, R., Hillerich, B., San Francisco, B., Solbiati, J., Steves, A., Brown, S., Akiva, E., Barber, A., Seidel, R. D., Babbitt, P. C., Almo, S. C., Gerlt, J. A., and Jacobson, M. P. (2014) Prediction and characterization of enzymatic activities guided by sequence similarity and genome neighborhood networks. *Elife 3*, e03275.

DOI: 10.1021/acs.biochem.5b00240
Biochemistry 2015, 54, 3009−3023